Measurement of the B^{0}→D^{*}^{-}π^{+}π^{-}π^{+} branching fraction

J. P. Lees *et al.* (BABAR Collaboration)

Phys. Rev. D **94**, 091101 — Published 15 November 2016

DOI: 10.1103/PhysRevD.94.091101

BABAR-PUB-16/015
SLAC-PUB-16822
arXiv1609:06802 [hep-ex]

Measurement of the $B^0 \to D^{*-}\pi^+\pi^-\pi^+$ branching fraction

J. P. Lees,[1] V. Poireau,[1] V. Tisserand,[1] E. Grauges,[2] A. Palano,[3] G. Eigen,[4] D. N. Brown,[5] Yu. G. Kolomensky,[5] H. Koch,[6] T. Schroeder,[6] C. Hearty,[7] T. S. Mattison,[7] J. A. McKenna,[7] R. Y. So,[7] V. E. Blinov[abc],[8] A. R. Buzykaev[a],[8] V. P. Druzhinin[ab],[8] V. B. Golubev[ab],[8] E. A. Kravchenko[ab],[8] A. P. Onuchin[abc],[8] S. I. Serednyakov[ab],[8] Yu. I. Skovpen[ab],[8] E. P. Solodov[ab],[8] K. Yu. Todyshev[ab],[8] A. J. Lankford,[9] J. W. Gary,[10] O. Long,[10] A. M. Eisner,[11] W. S. Lockman,[11] W. Panduro Vazquez,[11] D. S. Chao,[12] C. H. Cheng,[12] B. Echenard,[12] K. T. Flood,[12] D. G. Hitlin,[12] J. Kim,[12] T. S. Miyashita,[12] P. Ongmongkolkul,[12] F. C. Porter,[12] M. Röhrken,[12] Z. Huard,[13] B. T. Meadows,[13] B. G. Pushpawela,[13] M. D. Sokoloff,[13] L. Sun,[13,*] J. G. Smith,[14] S. R. Wagner,[14] D. Bernard,[15] M. Verderi,[15] F. Betti[ab],[16,†] D. Bettoni[a],[16] C. Bozzi[a],[16] R. Calabrese[ab],[16] G. Cibinetto[ab],[16] E. Fioravanti[ab],[16] I. Garzia[ab],[16] E. Luppi[ab],[16] V. Santoro[a],[16] A. Calcaterra,[17] R. de Sangro,[17] G. Finocchiaro,[17] S. Martellotti,[17] P. Patteri,[17] I. M. Peruzzi,[17] M. Piccolo,[17] M. Rotondo,[17] A. Zallo,[17] S. Passaggio,[18] C. Patrignani,[18,‡] B. Bhuyan,[19] U. Mallik,[20] C. Chen,[21] J. Cochran,[21] S. Prell,[21] H. Ahmed,[22] A. V. Gritsan,[23] N. Arnaud,[24] M. Davier,[24] F. Le Diberder,[24] A. M. Lutz,[24] G. Wormser,[24] D. J. Lange,[25] D. M. Wright,[25] J. P. Coleman,[26] E. Gabathuler,[26] D. E. Hutchcroft,[26] D. J. Payne,[26] C. Touramanis,[26] A. J. Bevan,[27] F. Di Lodovico,[27] R. Sacco,[27] G. Cowan,[28] Sw. Banerjee,[29] D. N. Brown,[29] C. L. Davis,[29] A. G. Denig,[30] M. Fritsch,[30] W. Gradl,[30] K. Griessinger,[30] A. Hafner,[30] K. R. Schubert,[30] R. J. Barlow,[31,§] G. D. Lafferty,[31] R. Cenci,[32] A. Jawahery,[32] D. A. Roberts,[32] R. Cowan,[33] R. Cheaib,[34] S. H. Robertson,[34] B. Dey[a],[35] N. Neri[a],[35] F. Palombo[ab],[35] L. Cremaldi,[36] R. Godang,[36,¶] D. J. Summers,[36] P. Taras,[37] G. De Nardo,[38] C. Sciacca,[38] G. Raven,[39] C. P. Jessop,[40] J. M. LoSecco,[40] K. Honscheid,[41] R. Kass,[41] A. Gaz[a],[42] M. Margoni[ab],[42] M. Posocco[a],[42] G. Simi[ab],[42] F. Simonetto[ab],[42] R. Stroili[ab],[42] S. Akar,[43] E. Ben-Haim,[43] M. Bomben,[43] G. R. Bonneaud,[43] G. Calderini,[43] J. Chauveau,[43] G. Marchiori,[43] J. Ocariz,[43] M. Biasini[ab],[44] E. Manoni[a],[44] A. Rossi[a],[44] G. Batignani[ab],[45] S. Bettarini[ab],[45] M. Carpinelli[ab],[45,**] G. Casarosa[ab],[45] M. Chrzaszcz[a],[45] F. Forti[ab],[45] M. A. Giorgi[ab],[45] A. Lusiani[ac],[45] B. Oberhof[ab],[45] E. Paoloni[ab],[45] M. Rama[a],[45] G. Rizzo[ab],[45] J. J. Walsh[a],[45] A. J. S. Smith,[46] F. Anulli[a],[47] R. Faccini[ab],[47] F. Ferrarotto[a],[47] F. Ferroni[ab],[47] A. Pilloni[ab],[47] G. Piredda[a],[47,††] C. Bünger,[48] S. Dittrich,[48] O. Grünberg,[48] M. Heß,[48] T. Leddig,[48] C. Voß,[48] R. Waldi,[48] T. Adye,[49] F. F. Wilson,[49] S. Emery,[50] G. Vasseur,[50] D. Aston,[51] C. Cartaro,[51] M. R. Convery,[51] J. Dorfan,[51] W. Dunwoodie,[51] M. Ebert,[51] R. C. Field,[51] B. G. Fulsom,[51] M. T. Graham,[51] C. Hast,[51] W. R. Innes,[51] P. Kim,[51] D. W. G. S. Leith,[51] S. Luitz,[51] V. Luth,[51] D. B. MacFarlane,[51] D. R. Muller,[51] H. Neal,[51] B. N. Ratcliff,[51] A. Roodman,[51] M. K. Sullivan,[51] J. Va'vra,[51] W. J. Wisniewski,[51] M. V. Purohit,[52] J. R. Wilson,[52] A. Randle-Conde,[53] S. J. Sekula,[53] M. Bellis,[54] P. R. Burchat,[54] E. M. T. Puccio,[54] M. S. Alam,[55] J. A. Ernst,[55] R. Gorodeisky,[56] N. Guttman,[56] D. R. Peimer,[56] A. Soffer,[56] S. M. Spanier,[57] J. L. Ritchie,[58] R. F. Schwitters,[58] J. M. Izen,[59] X. C. Lou,[59] F. Bianchi[ab],[60] F. De Mori[ab],[60] A. Filippi[a],[60] D. Gamba[ab],[60] L. Lanceri,[61] L. Vitale,[61] F. Martinez-Vidal,[62] A. Oyanguren,[62] J. Albert,[63] A. Beaulieu,[63] F. U. Bernlochner,[63] G. J. King,[63] R. Kowalewski,[63] T. Lueck,[63] I. M. Nugent,[63] J. M. Roney,[63] N. Tasneem,[63] T. J. Gershon,[64] P. F. Harrison,[64] T. E. Latham,[64] R. Prepost,[65] and S. L. Wu[65]

(The *BABAR* Collaboration)

[1] *Laboratoire d'Annecy-le-Vieux de Physique des Particules (LAPP), Université de Savoie, CNRS/IN2P3, F-74941 Annecy-Le-Vieux, France*
[2] *Universitat de Barcelona, Facultat de Fisica, Departament ECM, E-08028 Barcelona, Spain*
[3] *INFN Sezione di Bari and Dipartimento di Fisica, Università di Bari, I-70126 Bari, Italy*
[4] *University of Bergen, Institute of Physics, N-5007 Bergen, Norway*
[5] *Lawrence Berkeley National Laboratory and University of California, Berkeley, California 94720, USA*
[6] *Ruhr Universität Bochum, Institut für Experimentalphysik 1, D-44780 Bochum, Germany*
[7] *University of British Columbia, Vancouver, British Columbia, Canada V6T 1Z1*
[8] *Budker Institute of Nuclear Physics SB RAS, Novosibirsk 630090[a], Novosibirsk State University, Novosibirsk 630090[b], Novosibirsk State Technical University, Novosibirsk 630092[c], Russia*
[9] *University of California at Irvine, Irvine, California 92697, USA*
[10] *University of California at Riverside, Riverside, California 92521, USA*
[11] *University of California at Santa Cruz, Institute for Particle Physics, Santa Cruz, California 95064, USA*
[12] *California Institute of Technology, Pasadena, California 91125, USA*

[13]University of Cincinnati, Cincinnati, Ohio 45221, USA
[14]University of Colorado, Boulder, Colorado 80309, USA
[15]Laboratoire Leprince-Ringuet, Ecole Polytechnique, CNRS/IN2P3, F-91128 Palaiseau, France
[16]INFN Sezione di Ferrara[a]; Dipartimento di Fisica e Scienze della Terra, Università di Ferrara[b], I-44122 Ferrara, Italy
[17]INFN Laboratori Nazionali di Frascati, I-00044 Frascati, Italy
[18]INFN Sezione di Genova, I-16146 Genova, Italy
[19]Indian Institute of Technology Guwahati, Guwahati, Assam, 781 039, India
[20]University of Iowa, Iowa City, Iowa 52242, USA
[21]Iowa State University, Ames, Iowa 50011, USA
[22]Physics Department, Jazan University, Jazan 22822, Kingdom of Saudi Arabia
[23]Johns Hopkins University, Baltimore, Maryland 21218, USA
[24]Laboratoire de l'Accélérateur Linéaire, IN2P3/CNRS et Université Paris-Sud 11,
Centre Scientifique d'Orsay, F-91898 Orsay Cedex, France
[25]Lawrence Livermore National Laboratory, Livermore, California 94550, USA
[26]University of Liverpool, Liverpool L69 7ZE, United Kingdom
[27]Queen Mary, University of London, London, E1 4NS, United Kingdom
[28]University of London, Royal Holloway and Bedford New College, Egham, Surrey TW20 0EX, United Kingdom
[29]University of Louisville, Louisville, Kentucky 40292, USA
[30]Johannes Gutenberg-Universität Mainz, Institut für Kernphysik, D-55099 Mainz, Germany
[31]University of Manchester, Manchester M13 9PL, United Kingdom
[32]University of Maryland, College Park, Maryland 20742, USA
[33]Massachusetts Institute of Technology, Laboratory for Nuclear Science, Cambridge, Massachusetts 02139, USA
[34]McGill University, Montréal, Québec, Canada H3A 2T8
[35]INFN Sezione di Milano[a]; Dipartimento di Fisica, Università di Milano[b], I-20133 Milano, Italy
[36]University of Mississippi, University, Mississippi 38677, USA
[37]Université de Montréal, Physique des Particules, Montréal, Québec, Canada H3C 3J7
[38]INFN Sezione di Napoli and Dipartimento di Scienze Fisiche,
Università di Napoli Federico II, I-80126 Napoli, Italy
[39]NIKHEF, National Institute for Nuclear Physics and High Energy Physics, NL-1009 DB Amsterdam, The Netherlands
[40]University of Notre Dame, Notre Dame, Indiana 46556, USA
[41]Ohio State University, Columbus, Ohio 43210, USA
[42]INFN Sezione di Padova[a]; Dipartimento di Fisica, Università di Padova[b], I-35131 Padova, Italy
[43]Laboratoire de Physique Nucléaire et de Hautes Energies,
IN2P3/CNRS, Université Pierre et Marie Curie-Paris6,
Université Denis Diderot-Paris7, F-75252 Paris, France
[44]INFN Sezione di Perugia[a]; Dipartimento di Fisica, Università di Perugia[b], I-06123 Perugia, Italy
[45]INFN Sezione di Pisa[a]; Dipartimento di Fisica,
Università di Pisa[b]; Scuola Normale Superiore di Pisa[c], I-56127 Pisa, Italy
[46]Princeton University, Princeton, New Jersey 08544, USA
[47]INFN Sezione di Roma[a]; Dipartimento di Fisica,
Università di Roma La Sapienza[b], I-00185 Roma, Italy
[48]Universität Rostock, D-18051 Rostock, Germany
[49]Rutherford Appleton Laboratory, Chilton, Didcot, Oxon, OX11 0QX, United Kingdom
[50]CEA, Irfu, SPP, Centre de Saclay, F-91191 Gif-sur-Yvette, France
[51]SLAC National Accelerator Laboratory, Stanford, California 94309 USA
[52]University of South Carolina, Columbia, South Carolina 29208, USA
[53]Southern Methodist University, Dallas, Texas 75275, USA
[54]Stanford University, Stanford, California 94305, USA
[55]State University of New York, Albany, New York 12222, USA
[56]Tel Aviv University, School of Physics and Astronomy, Tel Aviv, 69978, Israel
[57]University of Tennessee, Knoxville, Tennessee 37996, USA
[58]University of Texas at Austin, Austin, Texas 78712, USA
[59]University of Texas at Dallas, Richardson, Texas 75083, USA
[60]INFN Sezione di Torino[a]; Dipartimento di Fisica, Università di Torino[b], I-10125 Torino, Italy
[61]INFN Sezione di Trieste and Dipartimento di Fisica, Università di Trieste, I-34127 Trieste, Italy
[62]IFIC, Universitat de Valencia-CSIC, E-46071 Valencia, Spain
[63]University of Victoria, Victoria, British Columbia, Canada V8W 3P6
[64]Department of Physics, University of Warwick, Coventry CV4 7AL, United Kingdom
[65]University of Wisconsin, Madison, Wisconsin 53706, USA

Using a sample of $(470.9 \pm 2.8) \times 10^6$ $B\overline{B}$ pairs, we measure the decay branching fraction $\mathcal{B}(B^0 \to D^{*-}\pi^+\pi^-\pi^+) = (7.26 \pm 0.11 \pm 0.31) \times 10^{-3}$, where the first uncertainty is statistical and the second is systematic. Our measurement will be helpful in studies of lepton universality by measuring $\mathcal{B}(B^0 \to D^{*-}\tau^+\nu_\tau)$ using $\tau^+ \to \pi^+\pi^-\pi^+\overline{\nu}_\tau$ decays, normalized to $\mathcal{B}(B^0 \to D^{*-}\pi^+\pi^-\pi^+)$.

PACS numbers: 13.20.He, 14.40.Nd

The *BABAR* Collaboration measured the branching fraction ratios for B semileptonic decays to D and D^*

$$\mathcal{R}^{(*)} = \frac{\mathcal{B}(\overline{B} \to D^{(*)}\tau^-\overline{\nu}_\tau)}{\mathcal{B}(\overline{B} \to D^{(*)}\ell^-\overline{\nu}_l)}, \quad (1)$$

where ℓ^- is an electron or a muon, to be in excess of standard model (SM) predictions [1]. The use of charge conjugate reactions is implied throughout this article. After combining the results for $\mathcal{R}$ and $\mathcal{R}^*$, the excess is inconsistent with lepton universality at the 3.4σ level. The Belle Collaboration [2] and the LHCb Collaboration [3] conducted similar measurements with comparable results. A measurement of $\mathcal{B}(B^0 \to D^{*-}\tau^+\nu_\tau)$ using $\tau^+ \to \pi^+\pi^-\pi^+\overline{\nu}_\tau$ decays, normalized to $\mathcal{B}(B^0 \to D^{*-}\pi^+\pi^-\pi^+)$, may yield the observation of a further deviation from the SM. Such a measurement has not been done before and may make use of a clean kinematic signature. This possibility relies in part on a measurement of $\mathcal{B}(B^0 \to D^{*-}\pi^+\pi^-\pi^+)$, for which the current world average value is $(7.0 \pm 0.8) \times 10^{-3}$ [4]. The LHCb Collaboration measured this value to be $(7.27 \pm 0.11(\text{stat.}) \pm 0.36(\text{syst.}) \pm 0.34(\text{norm.})) \times 10^{-3}$ [5], where the final uncertainty is due to using $B^0 \to D^{*-}\pi^+$ decays for normalization purposes. This measurement has not been included in the world average value as yet. In this article, we report on a measurement of $\mathcal{B}(B^0 \to D^{*-}\pi^+\pi^-\pi^+)$.

We use data recorded with the *BABAR* detector at the PEP-II asymmetric-energy e^+e^- collider at SLAC. The *BABAR* detector is described in detail elsewhere [6, 7]. The data sample corresponds to an integrated luminosity of 424.2 ± 1.8 fb^{-1} collected at the $\Upsilon(4S)$ resonance [8], which corresponds to the production of $(470.9 \pm 2.8) \times 10^6$ $B\overline{B}$ pairs. We use Monte Carlo (MC) simulations to understand background processes and signal reconstruction efficiencies. The EvtGen event generator [9] is used to simulate particle decays. This includes a sample of $e^+e^- \to q\overline{q}(\gamma)$ events, where q is a u, d, s, or c quark, with an equivalent luminosity of 2,589 fb^{-1} and a sample of $1,427 \times 10^6$ $B\overline{B}$ pairs. The detector response is simulated with the Geant4 [10] suite of programs.

We fully reconstruct the $B^0 \to D^{*-}\,\pi^+\,\pi^-\,\pi^+$ decay chain by adding the four-momenta of particle candidates. The D^{*-} mesons are reconstructed in the $D^{*-} \to \overline{D}^0\pi^-$ and $\overline{D}^0 \to K^+\pi^-$ final states. A $\overline{D}^0$ candidate is reconstructed from two charged-particle tracks, of which one is identified as a K^+ meson based on information obtained using the tracking and Cherenkov detectors. We require $\overline{D}^0$ candidates to have an invariant-mass value within $\pm 20\,\text{MeV}/c^2$ of the nominal $\overline{D}^0$ mass [4], which corresponds to 3 standard deviations in its mass resolution. Each $\overline{D}^0$ candidate is combined with a charged-particle track with momentum less than $0.45\,\text{GeV}/c$ in the e^+e^- center-of-mass (CM) frame to form a D^{*-} candidate. We require the difference between the reconstructed mass of the D^{*-} candidate and the reconstructed mass of the $\overline{D}^0$ candidate to lie between 0.1435 and $0.1475\,\text{GeV}/c^2$. The D^{*-} candidate is combined with three other charged-particle tracks to form a B^0 candidate. We do not explicitly apply particle identification to select charged pions, but assign the pion mass hypothesis to all tracks other than the K^+ daughter of the $\overline{D}^0$. All other reconstructed tracks and neutral clusters in the event are collectively referred to as the rest of the event (ROE). We use a neural network classifier [11] to suppress non-$B\overline{B}$ backgrounds. The classifier makes use of nine variables, each of which is calculated in the CM frame:

- the cosine of the angle between the B^0 candidate's thrust axis [12] and the beam axis;
- the sphericity [13] of the B^0 candidate;
- the thrust of the ROE;
- the sum over the ROE of p, where p is the magnitude of a particle's momentum;
- the sum over the ROE of $\frac{1}{2}(3\cos^2\theta - 1)p$, where θ is the polar angle of a particle's momentum;
- the cosine of the angle between the thrust axis of the B^0 candidate and the thrust axis of the ROE;
- the cosine of the angle between the sphericity axis of the B^0 candidate and the thrust axis of the ROE;
- the ratio of the second-order to zeroth-order Fox-Wolfram moment using all reconstructed particles [14];
- the cosine of the angle between the thrust axis calculated using all reconstructed particles and the beam axis.

Each of these nine variables contributes to separating B^0 decays from non-$B\overline{B}$ decays. We apply a selection on the output of the neural network classifier that rejects 69% of reconstructed signal candidates from non-$B\overline{B}$ decays, and retains 80% of correctly reconstructed B^0 candidates. Finally, we require the B^0 candidate to have a CM frame energy within $\pm 90\,\text{MeV}$ of $\sqrt{s}/2$, where $\sqrt{s}$

*Now at: Wuhan University, Wuhan 43072, China
†Also at: Laboratoire de l'Accélérateur Linéaire, F-91898 Orsay Cedex, France
‡Now at: Università di Bologna and INFN Sezione di Bologna, I-47921 Rimini, Italy
§Now at: University of Huddersfield, Huddersfield HD1 3DH, UK
¶Now at: University of South Alabama, Mobile, Alabama 36688, USA
**Also at: Università di Sassari, I-07100 Sassari, Italy
††Deceased

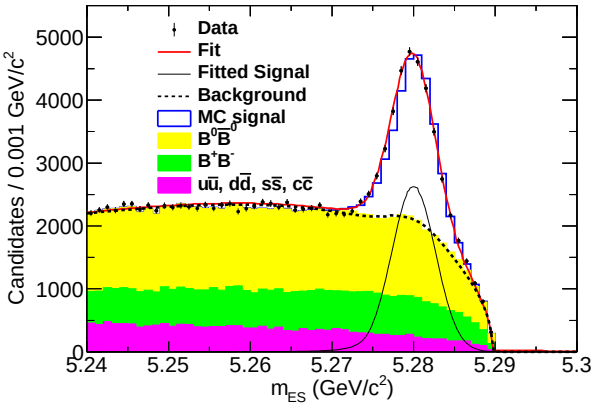

FIG. 1: (color online) The $m_{\rm ES}$ distribution of B^0 candidates for data (points), MC simulations (histograms), and the unbinned extended-maximum-likelihood fit to the data (curves). The MC distributions are shown as stacked histograms. The $B^0 \to D^{*-}D_s^+$ with $D_s^+ \to \pi^+\pi^-\pi^+$ decays are part of the MC signal. The MC signal contribution is normalized such that its stacked histogram has the same integral as the data. The components of the MC simulations and the fit are described in the legend. The $m_{\rm ES}$ peak of the MC signal is slightly above that of the data. This shift has a negligible effect on the signal yield.

is the nominal invariant-mass of the initial state. This corresponds to 4 standard deviations in the energy resolution. We retain all B^0 candidates that pass our selection criteria instead of selecting a best candidate for each event. In MC-simulated signal and background events that have at least one B^0 candidate passing all selection criteria, there are on average 1.57 and 1.37 B^0 candidates per event, respectively. We do not apply corrections to the number of B^0 candidates per event, as the B^0 candidate multiplicity in data is consistent with the weighted average of those in the signal and background simulation.

After applying all selection criteria, we determine the energy-substituted mass $m_{\rm ES} = \sqrt{s/4 - p_B^2}$ for the selected B^0 candidates, where p_B is the CM-frame momentum of a B^0. Figure 1 shows the $m_{\rm ES}$ distribution for the data and for MC-simulated events. The $m_{\rm ES}$ distribution of correctly reconstructed signal candidates has a peak near the B^0 mass.

The $m_{\rm ES}$ distribution of signal events is modeled using a Crystal Ball [15] probability density function (PDF), with cutoff and power-law parameters determined using MC-simulated events. We consider only B^0 candidates that are correctly reconstructed. We model the background $m_{\rm ES}$ distribution as follows. The non-peaking backgrounds from $e^+e^- \to q\overline{q}(\gamma)$ events and from $B\overline{B}$ pairs are modeled using an ARGUS function [16]. Each of the peaking backgrounds from B^+B^- and $B^0\overline{B}^0$ is modeled by a Gaussian distribution for which the normalization, mean, and width, are determined by a fit to the corresponding simulated event sample. We perform a one-dimensional unbinned extended-maximum-likelihood fit in order to estimate the number of signal candidates. We allow the mean and width parameters of the Crystal Ball function, the curvature parameter of the ARGUS function, and the normalization of the non-peaking background, to vary in the fit. The cutoff parameter for the ARGUS function is fixed to $\sqrt{s}/2$, and the peaking background PDF shapes and normalizations are fixed to their MC-estimated values. The peaking background contributions are estimated to be 590 ± 120 and 1450 ± 130 candidates from B^+B^- and $B^0\overline{B}^0$ decays, respectively; some originate from signal decays where one or more pion is misreconstructed even when there is a correctly reconstructed B^0 candidate. There is also a contribution from $B^+ \to D^{*-}X$ and $B^0 \to D^{*-}X$ decays, where X denotes any combination of π and ρ mesons other than $\rho^0\pi^+$ or $\pi^+\pi^-\pi^+$. The fit to the $m_{\rm ES}$ distribution shown in Fig. 1 results in a signal yield of 17800 ± 300.

The distribution for the MC signal peaks 0.2 MeV/c^2 higher in $m_{\rm ES}$ value than the data. This arises from a value of the simulated B^0 mass that is different from that found in Ref. [4]. We weight the simulated events in order to match the data mass peak and we repeat the measurement of the simulated efficiencies for the signal and the peaking background. The change is negligible and produces a negligible correction on the branching fraction measurement.

We define the signal region to be $5.273 < m_{\rm ES} < 5.285$ GeV/c^2, and a sideband region to be $5.240 < m_{\rm ES} < 5.270$ GeV/c^2. About 97.6% of signal events are contained within the signal region. To obtain the 3π invariant mass distribution for the signal events in Fig. 2, we subtract the events in the sideband region of the $m_{\rm ES}$ in Fig. 1, normalized to the fitted background component in the signal region, from the total 3π mass distribution. By integrating the dashed line in Fig. 1, we obtain 68883 events in the sideband-region and 24427 background events in the signal region. These values make use of the peaking background estimates described in the previous paragraph.

As expected from the branching fractions in Ref. [4], the main contribution comes from $a_1^+(1260)$ decays, and a contribution from the decay $D_s^+ \to \pi^+\pi^-\pi^+$ is also apparent. There is as well activity in the 1.7–1.9 GeV/c^2 region, which may be due to the $J^P = 0^-$ $\pi(1800)$ meson. The analysis of the a_1^+ region is complicated and will be the subject of a separate study.

The D_s^+ events result from the doubly-charmed decay $B^0 \to D^{*-}D_s^+$ in which the D_s^+ decays weakly to π^+ π^- π^+. Since the D_s^+ decay results from an entirely different B^0 decay mode, it represents a contamination of our $D^{*-}\pi^+\pi^-\pi^+$ sample. We remove the D_s^+ contribution by subtracting the events in the 1.9–2.0 GeV/c^2 region of the 3π invariant-mass distribution of Fig. 2 that exceed the interpolation of the bin contents in the 1.8–1.9 GeV/c^2 and 2.0–2.1 GeV/c^2 regions. The removed D_s^+ contribution amounts to 233 ± 63 events, and the remaining events in the 1.9–2.0 GeV/c^2 region total 326 ± 35.

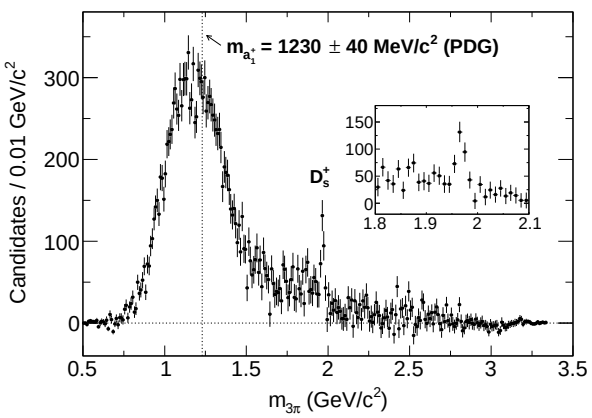

FIG. 2: The background-subtracted invariant-mass spectrum of the 3π system. The indicated mass value of the a_1^+ is obtained from Ref. [4]. The $B^0 \to D^{*-}D_s^+, D_s^+ \to \pi^+\pi^-\pi^+$ decay, which is removed in the final result, is visible in the spectrum. The spectrum is obtained prior to the efficiency correction. The inset shows the distribution around the D_s^+ region.

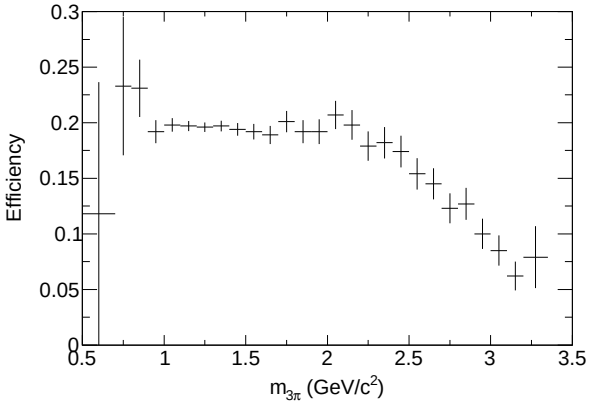

FIG. 3: The reconstruction efficiency as a function of 3π invariant-mass using MC-simulated events. The uncertainties are statistical.

TABLE I: Summary of systematic uncertainties. The uncertainties are assumed to be uncorrelated, and so are added in quadrature.

Source	Uncertainty (%)
Fit algorithm and peaking backgrounds	2.4
Track-finding	2.0
$\pi^+\pi^-\pi^+$ invariant-mass modeling	1.7
D^{*-} and $\overline{D}^0$ decay branching fractions	1.3
$\Upsilon(4S) \to B^0\overline{B}^0$ decay branching fraction	1.2
K^+ identification	1.1
Signal efficiency MC statistics	0.9
Sideband subtraction	0.7
$B\overline{B}$ counting	0.6
Total	4.3

We estimate the reconstruction efficiency as a function of 3π invariant-mass using MC-simulated events. This is shown in Fig. 3. Since we model the $m_{\rm ES}$ PDF of the signal only considering B^0 candidates that are correctly reconstructed, we apply exactly the same procedure of determining the signal yield in our study of the reconstruction efficiency in order to determine the branching fraction correctly. The efficiency of the decay channel $D^{*-}a_1^+$, where the a_1^+ decays to $\rho^0\pi^+$ and the ρ^0 to $\pi^+\pi^-$ was studied. The simulation assumes a mass of 1.230 GeV/c^2 and a width of 400 MeV for the a_1^+ [4]. The reconstruction efficiencies of $B^0 \to D^{*-}\rho^0\pi^+$ and $B^0 \to D^{*-}D_s^+$ decays are consistent with $B^0 \to D^{*-}a_1^+$ decays. Taking into account the efficiency as a function of the 3π mass, and removing the D_s^+ background, the total number of produced $B^0 \to D^{*-}\pi^+\pi^-\pi^+$ events is estimated to be 84400 ± 1200.

Table I summarizes the systematic uncertainties for this analysis. The uncertainties of our extended-maximum-likelihood fit algorithm and peaking backgrounds are estimated together by taking into account the uncertainties of the fixed parameters in the fit. The values we used are shown in Table II. These values are obtained entirely from studies of MC-simulated background samples. Therefore, we consider varying the mean and width of the $m_{\rm ES}$ distributions for the peaking B^+B^- and $B^0\overline{B}^0$ backgrounds, the number of $B^0\overline{B}^0$ and B^+B^- peaking background events, and the Crystal Ball PDF cutoff and power-law parameter values for the signal. These values are sampled from an eight-dimensional Gaussian function with means, widths, and correlations that correspond to the fit results for the PDF's for signal and peaking backgrounds from simulated events. The systematic uncertainty is taken as the standard deviation of the distribution of the number of signal events from an ensemble of fits, and is found to be 2.4%. The systematic uncertainty due to track-finding consists of two components: 1.54% for laboratory momenta less than 0.18 GeV/c, a region dominated by tracks from the decay $D^{*-} \to \overline{D}^0\pi^-$, and 0.26% for greater than this value [17]. The two components are added in quadrature. The pion from the $D^{*-} \to \overline{D}^0\pi^-$ decay has momentum less than 0.180 GeV/c 62% of the time. The corresponding fraction for other pions in the signal B^0 decay is 5%. The 3π invariant-mass of the D_s^+ contamination has the same mass location and width in the data and MC-simulated events. However, there are differences between the full reconstructed 3π invariant-mass spectrum for the data and that obtained from MC-simulated events. We studied the signal yield before and after reweighting the 3π invariant-mass spectrum in the MC-simulated events to match the data. The observed change due to the reweighting of the 3π mass distribution is 1.7%, which we assign as the associated systematic uncertainty. This also accounts for uncertainties in the relative contributions of the different decay modes and the mass and width of the a_1^+ reso-

TABLE II: Fit parameters obtained from MC-simulated events. These parameters are fixed to the central values in the signal extraction procedure. We perform a toy study where we simultaneously vary these by the quoted uncertainties (along with their correlations, which are not shown in the table) to study systematic effects on the signal yield.

Parameter	Value
B^+B^- peaking background $m_{\rm ES}$ Gaussian mean	5.2796 ± 0.0006 GeV/c^2
B^+B^- peaking background $m_{\rm ES}$ Gaussian width	0.0036 ± 0.0003 GeV/c^2
Number of B^+B^- peaking background	590 ± 120
$B^0\overline{B}^0$ peaking background $m_{\rm ES}$ Gaussian mean	5.2806 ± 0.0002 GeV/c^2
$B^0\overline{B}^0$ peaking background $m_{\rm ES}$ Gaussian width	0.0029 ± 0.0002 GeV/c^2
Number of $B^0\overline{B}^0$ peaking background	1450 ± 130
Signal's Crystal Ball PDF cutoff value	2.09 ± 0.08
Signal's Crystal Ball PDF power-law value	3.7 ± 0.5

nance. We use the D^{*-} and $\overline{D}^0$ decay branching fraction uncertainties from Ref. [4]. We use the value of $\mathcal{B}(\Upsilon(4S) \to B^0\overline{B}^0) = 0.486 \pm 0.006$ from Ref. [4] for the branching fraction of the decay $\Upsilon(4S) \to B^0\overline{B}^0$, which has a relative uncertainty of 1.2%. The kaon identification uncertainty is estimated by comparing the number of D^{*-} events in data and MC simulations with and without implementing identification requirements. According to dedicated studies using *BABAR* data control samples, we correct for kaon-identification efficiency differences between data and MC simulation by a factor of 0.978 ± 0.011, where the uncertainty is chosen to be half the difference from unity. The signal efficiency MC statistical uncertainty is 0.9%. Nominally, we subtract the 3π mass distribution in the sideband from that of the signal region. However, the 3π mass distribution of both peaking and non-peaking backgrounds in the signal region may not necessarily be the same as that in the sideband. To estimate the associated systematic uncertainty, we test the sideband subtraction procedure using only MC-simulated background events. After applying efficiency corrections to the resulting distribution, we obtain an integral of 571. Dividing this by the number of efficiency-corrected signal in the data, this translates to a 0.7% difference, which we assign as the associated systematic uncertainty. The number of B mesons produced is uncertain to 0.6% [8]. We studied the MC modeling of decay angle correlations, and found the associated systematic uncertainty to be negligible. As described earlier in the text, there is a peaking background contribution in the $m_{\rm ES}$ distribution due to signal events that are misreconstructed. The rate of this background depends on the branching fraction of signal events. Using our measured branching fraction value, we apply corrections to the expected number of $B^0\overline{B}^0$ peaking background and repeat the signal extraction procedure on the data. There is a small bias on the branching fraction value but it is negligible compared to the systematic uncertainty due to the other peaking backgrounds.

From the number of fitted signal events, corrected for efficiency and normalized to the total number of produced B^0 mesons in the data sample, and taking into account the D^{*-} and $\overline{D}^0$ branching fractions we derive $\mathcal{B}(B^0 \to D^{*-}\pi^+\pi^-\pi^+) = (7.26 \pm 0.11 \pm 0.31) \times 10^{-3}$, where the first uncertainty is statistical and the second systematic. The result is consistent with the current world average and is 2.4 times more precise. This result can be used as input for measurements of $\mathcal{R}^{(*)}$ using hadronic τ decays in the search for deviations from the SM. The inclusive branching fraction value without removing the D_s^+ contamination is $(7.37 \pm 0.11 \pm 0.31) \times 10^{-3}$.

We are grateful for the extraordinary contributions of our PEP-II colleagues in achieving the excellent luminosity and machine conditions that have made this work possible. The success of this project also relies critically on the expertise and dedication of the computing organizations that support *BABAR*. The collaborating institutions wish to thank SLAC for its support and the kind hospitality extended to them. This work is supported by the US Department of Energy and National Science Foundation, the Natural Sciences and Engineering Research Council (Canada), the Commissariat à l'Energie Atomique and Institut National de Physique Nucléaire et de Physique des Particules (France), the Bundesministerium für Bildung und Forschung and Deutsche Forschungsgemeinschaft (Germany), the Istituto Nazionale di Fisica Nucleare (Italy), the Foundation for Fundamental Research on Matter (The Netherlands), the Research Council of Norway, the Ministry of Education and Science of the Russian Federation, Ministerio de Economía y Competitividad (Spain), the Science and Technology Facilities Council (United Kingdom), and the Binational Science Foundation (U.S.-Israel). Individuals have received support from the Marie-Curie IEF program (European Union) and the A. P. Sloan Foundation (USA).

[1] J.P. Lees *et al.* (*BABAR* Collaboration), Phys. Rev. D **88**, 072012 (2013).

[2] M. Huschle *et al.* (Belle Collaboration), Phys. Rev. D **92**, 072014 (2015).

[3] R. Aaij *et al.* (LHCb Collaboration), Phys. Rev. Lett. **115**, 111803 (2015).

[4] K.A. Olive *et al.* (Particle Data Group), Chin. Phys. C **38**, 090001 (2014).

[5] R. Aaij *et al.* (LHCb Collaboration), Phys. Rev. D **87**, 092001 (2013).

[6] B. Aubert *et al.* (*BABAR* Collaboration), Nucl. Instr. Methods Phys. Res. Sect. A **479**, 1 (2002).

[7] B. Aubert *et al.* (*BABAR* Collaboration), Nucl. Instr. Methods Phys. Res. Sect. A **729**, 615 (2013).

[8] J. P. Lees *et al.* (*BABAR* Collaboration), Nucl. Instr. Methods Phys. Res. Sect. A **726**, 203 (2013).

[9] D. J. Lange, Nucl. Instr. Methods Phys. Res. Sect. A **462**, 152 (2001).

[10] S. Agostinelli *et al.* (Geant4 Collaboration), Nucl. Instr. Methods Phys. Res. Sect. A **506**, 250 (2003).

[11] A. Höcker *et al.*, PoS ACAT, 040 (2007), arXiv:physics/0703039.

[12] S. Brandt *et al.*, Phys. Lett. **12**, 57 (1964).

[13] J. Bjorken and S. Brodsky, Phys. Rev. D **1**, 1416 (1970).

[14] G. C. Fox and S. Wolfram, Nucl. Phys. B **149**, 413 (1979).

[15] M. J. Oreglia, Ph.D. thesis, SLAC, Report No. SLAC-R-236, 1980; J. E. Gaiser, Ph.D. thesis, SLAC, Report No. SLAC-R-255, 1982; T. Skwarnicki, Ph.D. thesis, INP and DESY, Report No. DESY-F31-86-02, 1986.

[16] H. Albrecht *et al.* (ARGUS Collaboration), Phys. Lett. B **241**, 278 (1990).

[17] T. Allmendinger *et al.*, Nucl. Instr. Methods Phys. Res. Sect. A **704**, 44 (2013).